Multiclass Recognition and Part Localization with Humans in the Loop

Catherine Wah[†] Steve Branson[†]
[†]Department of Computer Science and Engineering
University of California, San Diego
{cwah,sbranson,sjb}@cs.ucsd.edu

Pietro Perona[‡] Serge Belongie[†]
[‡]Department of Electrical Engineering
California Institute of Technology
perona@caltech.edu

Abstract

We propose a visual recognition system that is designed for fine-grained visual categorization. The system is composed of a machine and a human user. The user, who is unable to carry out the recognition task by himself, is interactively asked to provide two heterogeneous forms of information: clicking on object parts and answering binary questions. The machine intelligently selects the most informative question to pose to the user in order to identify the object's class as quickly as possible. By leveraging computer vision and analyzing the user responses, the overall amount of human effort required, measured in seconds, is minimized. We demonstrate promising results on a challenging dataset of uncropped images, achieving a significant average reduction in human effort over previous methods.

1. Introduction

Vision researchers have become increasingly interested in recognition of parts [2, 8, 21], attributes [6, 11, 12], and fine-grained categories (*e.g.* specific species of birds, flowers, or insects) [1, 3, 14, 15]. Beyond traditionally studied basic-level categories, these interests have led to progress in transfer learning and learning from fewer training examples [7, 8, 10, 15, 21], larger scale computer vision algorithms that share processing between tasks [15, 16], and new methodologies for data collection and annotation [2, 4].

Parts, attributes, and fine-grained categories push the limits of human expertise and are often inherently ambiguous concepts. For example, perception of the precise location of a particular part (such as a bird's beak) can vary from person to person, as does perception of whether or not an object is shiny. Fine-grained categories are usually recognized only by experts (*e.g.* the average person cannot recognize a Myrtle Warbler), while one can recognize immediately basic categories like cows and bottles.

We propose a key conceptual simplification: that humans and computers alike should be treated as valuable but ultimately imperfect sources of information. Humans are able to detect and broadly categorize objects, even when they do not recognize them, as well as carry out simple measurements such as telling color and shape; human errors arise primarily because (1) people have limited experiences and memory, and (2) people have subjective and perceptual differences. In contrast, computers can run identical pieces of software and aggregate large databases of information. They excel at memory-based problems like recognizing movie posters but struggle at detecting and recognizing objects that are non-textured, immersed in clutter, or highly shape-deformable.

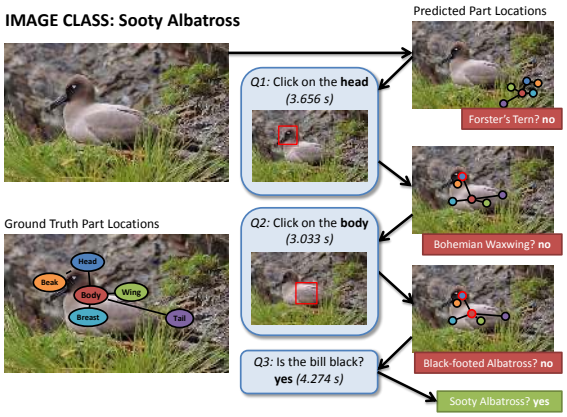

Figure 1. Our system can query the user for input in the form of binary attribute questions or part clicks. In this illustrative example, the system provides an estimate for the pose and part locations of the object at each stage. Given a user-clicked location of a part, the probability distributions for locations of the other parts in each pose will adjust accordingly. The rightmost column depicts the maximum likelihood estimate for part locations.

In order to achieve a unified treatment of humans and computers, we introduce models and algorithms that account for errors and inaccuracies of vision algorithms (part localization, attribute detection, and object classification) and ambiguities in multiple forms of human feedback (perception of part locations, attribute values, and class labels). The strengths and weaknesses of humans and computers for

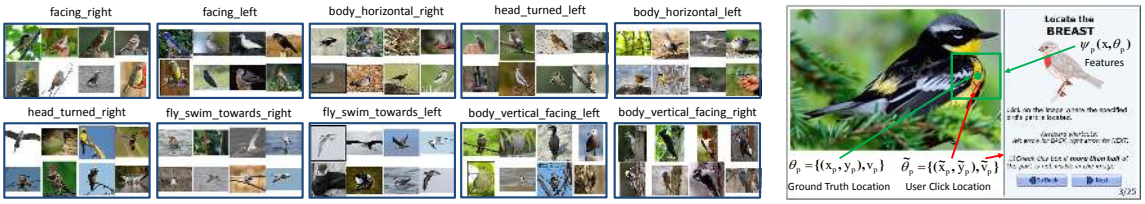

(a) Pose clusters

(b) User interface for part locations input

Figure 2. 2(a) Images in our dataset are clustered by k-means on the spatial offsets of part locations from parent part locations. Semantic labels of clusters were manually assigned by visual inspection. Left/right orientation is in reference to the image. 2(b) The user clicks on his/her perceived location of the breast $(\tilde{x}_p, \tilde{y}_p)$, which is shown as a red X and is assumed to be near the ground truth location (x_p, y_p). The user also can click a checkbox indicating part visibility $\tilde{v}_p$. Features $\psi_p(x, \theta_p)$ can be extracted from a box around θ_p.

these modalities are combined using a single principled objective function: minimizing the expected amount of time to complete a given classification task.

Consider for example different types of human annotation tasks in the domain of bird species recognition. For the task "*Click on the beak*," the location a human user clicks is a noisy representation of the ground truth location of the beak. It may not in isolation solve any single recognition task; however, it provides information that is useful to a machine vision algorithm for localizing other parts of the bird, measuring attributes (*e.g.* cone-shaped), recognizing actions (*e.g.* eating or flying), and ultimately recognizing the bird species. The answer to the question "*Is the belly striped?*" similarly provides information towards recognizing a variety of bird species. Each type of annotation takes a different amount of human time to complete and provides varying amounts of information.

Our models and algorithms combine all such sources of information into a single principled framework. We have implemented a practical real-time system[1] for bird species identification on a dataset of over 200 categories. Recognition and pose registration can be achieved automatically using computer vision; the system can also incorporate human feedback when computer vision is unsuccessful by intelligently posing questions to human users (see Figure 1).

The contributions of this paper are: (1) We introduce models and algorithms for object detection, part localization, and category recognition that scale efficiently to large numbers of categories. Our algorithms can localize and classify objects on a 200-class dataset in a fraction of a second, using part and attribute detectors that are shared among classes. (2) We introduce a formal model for evaluating the usefulness of different types of human input that takes into account varying levels of human error, time spent, and informativeness in a multiclass or multitask setting. We introduce fast algorithms that are able to predict the informativeness of 312 binary questions and 13 part click questions in a fraction of a second. All such computer vision algorithms, forms of user input, and question selection techniques are combined into an integrated framework. (3) We present a thorough experimental comparison of a number of methods for optimizing human input.

The structure of the paper is as follows: In Section 2, we review related work. We define the problem and describe the algorithm in Sections 3 and 4. In Section 5 we discuss implementation details, in Section 6 we present empirical results, and finally in Section 7 we discuss future work.

2. Related Work

Our work extends prior work by Branson *et al.* [3], who introduced a system combining human interaction with computer vision that was applied to bird species classification. They used an information-theoretic framework to intelligently select attribute questions such as "*Is the belly spotted?*", "*Is the wing white?*", *etc.* to identify the true bird species as quickly as possible. Our work has 3 main differences: (1) While [3] used non-localized computer vision methods based on bag-of-words features extracted from the entire image, we use localized part and attribute detectors. Thus [3] relied on experiments with test images cropped by ground truth bounding boxes; in contrast, our experiments are performed on uncropped images in unconstrained environments. (2) Whereas [3] incorporated only one type of user input – binary questions pertaining to attributes – we allow heterogeneous forms of user input including user-clicked part locations. Users can click on any pixel location in an image, introducing significant algorithmic and computational challenges as we must reason over hundreds of thousands of possible click point and part locations. (3) Whereas [3] measured human effort in terms of the total number of questions asked, we introduce an extended question selection criterion that factors in the expected amount of human time needed to answer each type of question.

A number of papers have recently addressed fine-grained categorization [1, 3, 13, 14, 15, 22]. One important differ-

[1] See http://visipedia.org/ for a demo of our system.

ence between this paper and prior work is that we use localized computer vision algorithms based on part and attribute detectors (in contrast, [3, 13, 14, 15] rely on bag-of-words methods). The differences between fine-grained categories are subtle, such that it is likely that lossy representations such as bag-of-words are insufficient. Bird field guides [19] suggest that humans use strongly localized methods based on parts and attributes to perform bird species recognition, justifying our approach. Also, we introduce an extended version of the CUB-200 dataset [18] that consists of 200 bird species and nearly $12,000$ images, each of which is labeled with part locations and attribute annotations (example images are shown in Figure 2(a)). Additional discussion of related work covered in [3] is not revisited here.

Our integrated approach builds on two areas in computer vision: part-based models and attribute-based learning, which have both been explored in depth in other works. Specifically, we use a part representation similar to a Felzenszwalb-style deformable part model [8, 9] (sliding window HOG-based part detectors fused with tree-structured spatial dependencies). Whereas most attribute-based methods [6, 12] use non-localized classifiers, [5, 20] incorporate object or part-level localization with attribute detectors. Our methods differ from earlier work on parts and attributes by (1) the specific combination of a Felzenszwalb-style deformable part model with localized attribute detectors, (2) the additional ability to combine part and attribute models with different types of user input, and (3) the deployment of such methods on a dataset of larger scale, localizing 200 object classes, 13 parts, 11 aspects, and 312 binary attributes in a fraction of a second.

3. Framework for Visual Recognition

In this section, we introduce a principled framework for integrating part-based detectors, multi-class categorization algorithms, and different types of human feedback into a common probabilistic model. We also introduce efficient algorithms for inferring and updating object class and localization predictions as additional user input is obtained. We begin by formally defining the problem.

3.1. Problem Definition and Notation

Given an image x, our goal is to predict an object class from a set of C possible classes (*e.g.* Myrtle Warbler, Blue Jay, Indigo Bunting) within a common basic-level category (*e.g.* Birds). We assume that the C classes fall within a reasonably homogeneous basic-level category such as birds that can be represented using a common vocabulary of P parts (*e.g.* head, belly, wing), and A attributes (*e.g.* cone-shaped beak, white belly, striped breast). We use a class-attribute model based on the direct-attribute model of Lampert et al. [12], where each class $c \in 1...C$ is represented using a unique, deterministic vector of attribute memberships $\mathbf{a}^c = [a_1^c ... a_A^c]$, $a_i^c \in 0, 1$. We extend this model to include part localized attributes, such that each attribute $a \in 1...A$ can optionally be associated with a part $\text{part}(a) \in 1...P$ (*e.g.* the attributes *white belly* and *striped belly* are both associated with the part belly). In this case, we express the set of all ground truth part locations for a particular object as $\Theta = \{\theta_1 ... \theta_P\}$, where the location θ_p of a particular part p is represented as an x_p, y_p image location, a scale s_p, and an aspect v_p (*e.g.* side view left, side view right, frontal view, not visible, *etc.*):

$$\theta_p = \{x_p, y_p, s_p, v_p\}. \quad (1)$$

Note that the special aspect *not visible* is used to handle parts that are occluded or self-occluded.

We can optionally combine our computer vision algorithms with human input, by intelligently querying user input at runtime. A human is capable of providing two types of user input which indirectly provide information relevant for predicting the object's class: mouse click locations $\tilde{\theta}_p$ and attribute question answers $\tilde{a}_i$. The random variable $\tilde{\theta}_p$ represents a user's input of the part location θ_p, which may differ from user to user due to both clicking inaccuracies and subjective differences in human perception (Figure 2(b)). Similarly, $\tilde{a}_i$ is a random variable defining a user's perception of the attribute value a_i.

We assume a pool of $A + P$ possible questions that can be posed to a human user $\mathcal{Q} = \{q_1 ... q_A, q_{A+1} ... q_{A+P}\}$, where the first A questions query $\tilde{a}_i$ and the remaining P questions query $\tilde{\theta}_p$. Let $\mathcal{A}_j$ be the set of possible answers to question q_j. At each time step t, our algorithm considers the visual content of the image and the current history of question responses to estimate a distribution over the location of each part, predict the probability of each class, and intelligently select the next question to ask $q_{j(t)}$. A user provides the response $u_{j(t)}$ to a question $q_{j(t)}$, which is the value of $\tilde{\theta}_p$ or $\tilde{a}_i$ for part location or attribute questions, respectively. The set of all user responses up to timestep t is denoted by the symbol $U^t = \{u_{j(1)} ... u_{j(t)}\}$. We assume that the user is consistent in answering questions and therefore the same question is never asked twice.

3.1.1 Probabilistic Model

Our probabilistic model incorporating both computer vision and human user responses is summarized in Figure 3(b). Our goal is to estimate the probability of each class given an arbitrary collection of user responses U^t and observed image pixels x:

$$p(c|U^t, x) = \frac{p(\mathbf{a^c}, U^t|x)}{\sum_c p(\mathbf{a^c}, U^t|x)}, \quad (2)$$

which follows from the assumption of unique, class-deterministic attribute memberships $\mathbf{a}^c$ [12]. We can in-

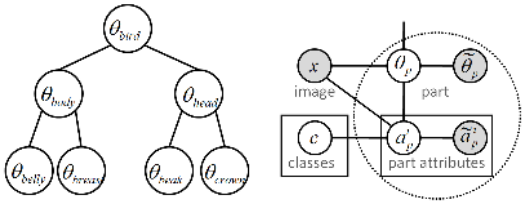

(a) Part Model (b) Part-Attribute Model

Figure 3. **Probabilistic Model.** 3(a): The spatial relationship between parts has a hierarchical independence structure. 3(b): Our model employs attribute estimators, where part variables θ_p are connected using the hierarchical model shown in 3(a).

corporate localization information Θ into the model by integrating over all possible assignments to part locations

$$p(\mathbf{a}^c, U^t|x) = \int_{\Theta} p(\mathbf{a}^c, U^t, \Theta|x) d\Theta. \quad (3)$$

We can write out each component of Eq 3 as

$$p(\mathbf{a}^c, U^t, \Theta|x) = p(\mathbf{a}^c|\Theta, x)p(\Theta|x)p(U^t|\mathbf{a}^c, \Theta, x) \quad (4)$$

where $p(\mathbf{a}^c|\Theta, x)$ is the response of a set of attribute detectors evaluated at locations Θ, $p(\Theta|x)$ is the response of a part-based detector, and $p(U^t|\mathbf{a}^c, \Theta, x)$ models the way users answer questions. We describe each of these probability distributions in Sections 3.2.1, 3.2.2, and 3.3 respectively and describe inference procedures for evaluating Eq 3 efficiently in Section 3.4.

3.2. Computer Vision Model

As described in Eq 4, we require two basic types of computer vision algorithms: one that estimates attribute probabilities $p(\mathbf{a}^c|\Theta, x)$ on a particular set of predicted part locations Θ, and another that estimates part location probabilities $p(\Theta|x)$.

3.2.1 Attribute Detection

Using the independence assumptions depicted in Figure 3(b), we can write the probability

$$p(\mathbf{a}^c|\Theta, x) = \prod_{a_i^c \in \mathbf{a}^c} p(a_i^c|\theta_{\text{part}(a_i)}, x). \quad (5)$$

Given a training set with labeled part locations $\theta_{\text{part}(a_i)}$, one can use standard computer vision techniques to learn an estimator for each $p(a_i|\theta_{\text{part}(a_i)}, x)$. In practice, we train a separate binary classifier for each attribute, extracting localized features from the ground truth location $\theta_{\text{part}(a_i)}$. As in [12], we convert attribute classification scores $z_i = f_a(x; \text{part}(a_i))$ to probabilities by fitting a sigmoid function $\sigma(\gamma_a z_i)$ and learning the sigmoid parameter γ_a using cross-validation. When $v_{\text{part}(a_i)} =$ *not visible*, we assume the attribute detection score is zero.

3.2.2 Part Detection

We use a pictorial structure to model part relationships (see Figure 3(a)), where parts are arranged in a tree-structured graph $T = (V, E)$. Our part model is a variant of the model used by Felzenszwalb et al. [8], which models the detection score $g(x; \Theta)$ as a sum over unary and pairwise potentials $\log(p(\Theta|x)) \propto g(x; \Theta)$ with

$$g(x; \Theta) = \sum_{p=1}^{P} \psi(x; \theta_p) + \sum_{(p,q) \in E} \lambda(\theta_p, \theta_q) \quad (6)$$

where each unary potential $\psi(x; \theta_p)$ is the response of a sliding window detector, and each pairwise score $\lambda(\theta_p, \theta_q)$ encodes a likelihood over the relative displacement between adjacent parts. We use the same learning algorithms and parametrization of each term in Eq 6 as in [23]. Here, parts and aspects are semantically defined, multiple aspects are handled using mixture models, and weight parameters for appearance and spatial terms are learned jointly using a structured SVM [17]. After training, we convert detection scores to probabilities $p(\Theta|x) \propto \exp(\gamma g(x; \Theta))$, where γ is a scaling parameter that is learned using cross-validation.

3.3. User Model

Readers interested in a computer-vision-only system with no human-in-the-loop can skip to Section 3.4. We assume that the probability of a set of user responses U^t can be expressed in terms of user responses that pertain to part click locations $U_\Theta^t \subseteq U^t$ and user responses that pertain to attribute questions $U_a^t \subseteq U^t$. We assume a user's perception of the location of a part $\tilde{\theta}_p$ depends only on the ground truth location of that part θ_p, and a user's perception of an attribute $\tilde{a}_i$ depends only on the ground truth attribute a_i^c:

$$p(U^t|\mathbf{a}^c, \Theta, x) = \left(\prod_{p \in U_\Theta^t} p(\tilde{\theta}_p|\theta_p) \right) \left(\prod_{\tilde{a}_i \in U_a^t} p(\tilde{a}_i|a_i^c) \right). \quad (7)$$

We describe our methods for estimating $p(\tilde{\theta}_p|\theta_p)$ and $p(\tilde{a}_i|a_i^c)$ in Sections 3.3.1 and 3.3.2 respectively.

3.3.1 Modeling User Click Responses

Our interface for collecting part locations is shown in Figure 2(b). We represent a user click response as a triplet $\tilde{\theta}_p = \{\tilde{x}_p, \tilde{y}_p, \tilde{v}_p\}$, where $(\tilde{x}_p, \tilde{y}_p)$ is a point that the user clicks with the mouse and $\tilde{v}_p \in \{$*visible*, *not visible*$\}$ is a binary variable indicating presence/absence of the part.

Note that the user click response $\tilde{\theta}_p$ models only part location and visibility, whereas the true part location θ_p also includes scale and aspect. This is done in order to keep the user interface as intuitive as possible. On the other hand, incorporating scale and aspect in the true model is extremely

important – the relative offsets and visibility of parts in *left side view* and *right side view* will be dramatically different. We model a distribution over user click responses as

$$p(\tilde{\theta}_p|\theta_p) = p(\tilde{x}_p, \tilde{y}_p|x_p, y_p, s_p)p(\tilde{v}_p|v_p) \quad (8)$$

where the relative part click locations are Gaussian distributed $\left(\frac{\tilde{x}_p - x_p}{s_p}, \frac{\tilde{y}_p - y_p}{s_p}\right) \sim \mathcal{N}(\tilde{\mu}_p, \tilde{\sigma}_p^2)$, and each $p(\tilde{v}_p|v_p)$ is a separate binomial distribution for each possible value of v_p. The parameters of these distributions are estimated using a training set of pairs $(\theta_p, \tilde{\theta}_p)$. This model of user click responses results in a simple, intuitive user interface and still allows for a sophisticated and computationally efficient model of part localization (Section 3.4).

3.3.2 Attribute Question Responses

We use a model of attribute user responses similar to [3]. We estimate each $p(\tilde{a}_i|a_i)$ as a binomial distribution, with parameters learned using a training set of user attribute responses collected from MTurk. As in [3], we allow users to qualify their responses with a certainty parameter *guessing*, *probably*, or *definitely*, and we incorporate a Beta prior to improve robustness when training data is sparse.

3.4. Inference

We describe the inference procedure for estimating per-class probabilities $p(c|U^t, x)$ (Eq 2), which involves evaluating $\int_\Theta p(\mathbf{a}^c, U^t, \Theta|x)d\Theta$. While this initially seems very difficult, we note that all user responses $\tilde{a}_p^i$ and $\tilde{\theta}_p$ are observed values pertaining only to a single part, and attributes a^c are deterministic when conditioned on a particular choice of class c. If we run inference separately for each class c, all components of Eqs 5 and 7 can simply be mapped into the unary potential for a particular part. Evaluating Eq 2 exactly is computationally similar to evaluating a separate pictorial structure inference problem for each class.

On the other hand, when C is large, running C inference problems can be inefficient. In practice, we use a faster procedure which approximates the integral in Eq 3 as a sum over K strategically chosen sample points:

$$\begin{aligned}\int_\Theta & p(\mathbf{a}^c, U^t, \Theta|x)d\Theta \\ &\approx \sum_{k=1}^{K} p(U^t|\mathbf{a}^c, \Theta_k^t, x)p(\mathbf{a}^c|\Theta_k^t, x)p(\Theta_k^t|x) \quad (9)\\ &= p(U_a^t|\mathbf{a}^c)\sum_{k=1}^{K} p(\mathbf{a}^c|\Theta_k^t, x)p(U_\Theta^t|\Theta_k^t, x)p(\Theta_k^t|x).\end{aligned}$$

We select the sample set $\Theta_1^t \ldots \Theta_K^t$ as the set of all local maxima in the probability distribution $p(U_\Theta^t|\Theta)p(\Theta|x)$. The set of local maxima can be found using standard methods for maximum likelihood inference on pictorial structures and then running non-maximal suppression, where probabilities for each user click response $p(\tilde{\theta}_p|\theta_p)$ are first mapped into a unary potential $\psi(x; \theta_p, \tilde{\theta}_p)$ (see Eq 6)

$$\psi(x; \theta_p, \tilde{\theta}_p) = \psi(x; \theta_p) + \log p(\tilde{\theta}_p|\theta_p). \quad (10)$$

The inference step takes time linear in the number of parts and pixel locations[2] and is efficient enough to run in a fraction of a second with 13 parts, 11 aspects, and 4 scales. Inference is re-run each time we obtain a new user click response $\tilde{\theta}_p$, resulting in a new set of samples. Sampling assignments to part locations ensures that attribute detectors only have to be evaluated on K candidate assignments to part locations; this opens the door for more expensive categorization algorithms (such as kernelized methods) that do not have to be run in a sliding window fashion.

4. Selecting the Next Question

In this section, we introduce a common framework for predicting the informativeness of different heterogeneous types of user input (including binary questions and mouse click responses) that takes into account the expected level of human error, informativeness in a multitask setting, expected annotation time, and spatial relationships between different parts. Our method extends the expected information gain criterion described in [3].

Let $\mathrm{IG}_t(q_j)$ be the expected information gain $\mathrm{IG}(c; u_j|x, U^t)$ from asking a new question q_j:

$$\mathrm{IG}_t(q_j) = \sum_{u_j \in \mathcal{A}_j} p(u_j|x, U^t)\big(\mathrm{H}(U^t, u_j) - \mathrm{H}(U^t)\big) \quad (11)$$

$$\mathrm{H}(U^t) = -\sum_c p(c|x, U^t)\log p(c|x, U^t) \quad (12)$$

where $\mathrm{H}(U^t)$ is shorthand for the conditional class entropy $\mathrm{H}(c|x, U^t)$. Evaluating Eq 11 involves considering every possible user-supplied answer $u_j \in \mathcal{A}_j$ to that question, and recomputing class probabilities $p(c|x, U^t, u_j)$. For yes/no attribute questions (querying a variable $\tilde{a}_i$), this is computationally efficient because the number of possible answers is only two, and attribute response probabilities $p(U_a^t|\mathbf{a}^c)$ are assumed to be independent from ground truth part locations (see Eq 9).

4.1. Predicting Informativeness of Mouse Clicks

In contrast, for part click questions the number of possible answers to each question is equal to the number of pixel locations, and computing class probabilities requires solving a new inference problem (Section 3.4) for each such location, which quickly becomes computationally intractible.

[2] Maximum likelihood inference involves a bottom-up traversal of T, doing a distance transform operation [8] for each part in the tree (takes time $O(n)$ time in the number of pixels).

We use a similar approximation to the random sampling method described in Section 3.4. For a given part location question q_j, we wish to compute expected entropy:

$$E_{\tilde{\theta}_p}[\mathrm{H}(U^t, \tilde{\theta}_p)] \quad = \quad \sum_{\tilde{\theta}_p} p(\tilde{\theta}_p|x, U^t)\, \mathrm{H}(U^t, \tilde{\theta}_p). \quad (13)$$

This can be done by drawing K samples $\tilde{\theta}^t_{p1} ... \tilde{\theta}^t_{pK}$ from the distribution $p(\tilde{\theta}_p|x, U^t)$, then computing expected entropy

$$E_{\tilde{\theta}_p}[\mathrm{H}(U^t, \tilde{\theta}_p)] \approx \quad (14)$$
$$-\sum_{k=1}^{K} p(\tilde{\theta}_p|x, U^t) \sum_c p(c|x, U^t, \tilde{\theta}^t_{pk}) \log p(c|x, U^t, \tilde{\theta}^t_{pk}).$$

In this case, each sample $\tilde{\theta}^t_{pk}$ is extracted from a sample Θ^t_k (Section 3.4) and each $p(c|x, U^t, \tilde{\theta}^t_{pk})$ is approximated as a weighted average over samples $\Theta^t_1 ... \Theta^t_K$. The full question selection procedure is fast enough to run in a fraction of a second on a single CPU core when using 13 click questions and 312 binary questions.

4.2. Selecting Questions By Time

The expected information gain criterion (Eq 11) attempts to minimize the total number of questions asked. This is suboptimal as different types of questions tend to take more time to answer than others (*e.g.*, part click questions are usually faster than attribute questions). We include a simple adaptation that attempts to minimize the expected amount of human time spent. The information gain criterion $\mathrm{IG}_t(q_j)$ encodes the expected number of bits of information gained by observing the random variable u_j. We assume that there is some unknown linear relationship between bits of information and reduction in human time. The best question to ask is then the one with the largest ratio of information gain relative to the expected time to answer it:

$$q^*_{j(t+1)} = \arg\max_{q_j} \frac{\mathrm{IG}_t(q_j)}{\mathbb{E}[\mathrm{time}(u_j)]} \quad (15)$$

where $\mathbb{E}[\mathrm{time}(u_j)]$ is the expected amount of time required to answer a question q_j.

5. Implementation Details

In this section we describe the dataset used to perform experiments, provide implementation details on the types of features used, and describe the methodologies used to obtain pose information for training.

5.1. Extended CUB-200 Dataset

We extended the existing CUB-200 dataset [22] to form CUB-200-2011 [18], which includes roughly $11,800$ images, nearly double the previous total. Each image is annotated with 312 binary attribute labels and 15 part labels. We obtained a list of attributes from a bird field guide website [19] and selected the parts associated with those attributes for labeling. Five different MTurk workers provided part labels for each image by clicking on the image to designate the location or denoting part absence (Figure 2(b)). One MTurk worker answered attribute questions for each image, specifying response certainty with options *guessing*, *probably*, and *definitely*. They were also given the option *not visible* if the associated part with the attribute was not present. At test time, we simulated user responses in a similar manner to [3], randomly selecting a stored response for each posed question. Instead of using bounding box annotations to crop objects, we used full uncropped images, resulting in a significantly more challenging dataset than CUB-200 [22].

5.2. Attribute Features

For attribute detectors, we used simple linear classifiers based on histograms of vector-quantized SIFT and vector-quantized RGB features (each with 128 codewords) which were extracted from windows around the location of an associated part. We believe that significant improvements in classification performance could be gained by exploring more sophisticated features or learning algorithms.

5.3. Part Model

As in [8], the unary scores of our part detector are implemented using HOG templates parametrized by a vector of linear appearance weights w_{v_p} for each part and aspect. The pairwise scores are quadratic functions over the displacement between (x_p, y_p) and (x_q, y_q), parametrized by a vector of spatial weights w_{v_p, v_q} for each pose and pair of adjacent parts. For computational efficiency, we assume that the pose and scale parameters are defined on an object level, and thus inference simply involves running a separate sliding window detector for each scale and pose. The ground truth scale of each object is computed based on the size of the object's bounding box.

5.4. Pose Clusters

Because our object parts are labeled only with visibility, we clustered images using k-means on the spatial x- and y-offsets of the part locations from their parent part locations, normalized with respect to image dimensions; this approach handles relative part locations in a manner most similar to how we model part relationships (Section 3.2.2). Examples of images grouped by their pose cluster are shown in Figure 2(a). Semantic labels were assigned post hoc by visual inspection. The clustering, while noisy, reveals some underlying pose information that can be discovered by part presence and locations.

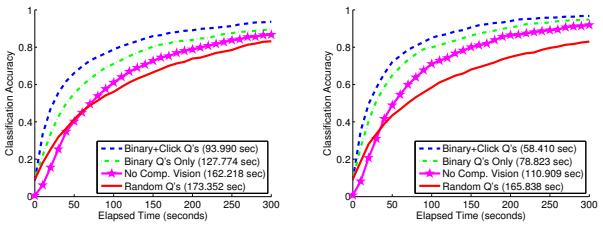

(a) Information gain criterion (b) Time criterion

Figure 4. Classification accuracy as a function of time when 4(a) maximizing expected information gain; and 4(b) minimizing amount of human labor, measured in time. Performance is measured as the average number of seconds to correctly classify an image (described in Section 6.1).

6. Experiments

6.1. Performance Metrics

We evaluate our approach using time as a measure of human effort needed to classify an object. This metric can be considered as a common quantifier for different forms of user input. Performance is determined by computing the average amount of time taken to correctly classify a test image. The computer presents images of the most likely class to the user, who will stop the system when the correct class is shown. This assumes that the user can validate the correct class with 100% accuracy, which may not be always possible. Future work will entail studying how well users can verify classification results.

6.2. Results

Using our criteria for question selection (Section 6.1) and our time-to-classification metric, we examine the average classification accuracy for: (1) our integrated approach combining localization/classification algorithms and part click and binary attribute questions; (2) using binary questions only with non-localized computer vision algorithms and expected information gain to select questions (representative of [3]); (3) using no computer vision; and (4) selecting questions at random. We follow with observations on how the addition of click questions affects performance and human effort required.

Question selection by time reduces human effort. By minimizing human effort with the time criterion, we are trading off between the expected information gain from a question response and the expected time to answer that question. Subsequently, we are able to classify images in 36.6 seconds less on average using both binary and click questions than if we only take into account expected information gain; however, the margin in performance gain between using and not using click questions is reduced.

We note that the average time to answer a part click question is 3.01 ± 0.26 seconds, compared to 7.64 ± 5.38 seconds for an attribute question; in this respect, part questions are more likely to be asked first.

Part localization improves performance. In Figure 4(a), we observe that by selecting the next question using our expected information gain criterion, average classification time using both types of user input versus only binary questions is reduced by 33.8 seconds on average. Compared to using no computer vision, we note an average reduction in human effort of over 40% (68.2 seconds).

Using the time criterion for selecting questions, the average classification time for a single image using both binary and click questions is 58.4 seconds. Asking binary questions only, the system takes an additional 20.4 seconds on average to correctly classify an image (Figure 4(b)). Using computer vision algorithms, we are able to consistently achieve higher average classification accuracy than using no computer vision at all, in the same period of time.

User responses drive up performance. There is a disparity in classification accuracy between evaluating attribute classifiers on ground truth locations (17.3%) versus predicted locations (10.3%); by using user responses to part click questions, we are able to overcome initial erroneous part detections and guide the system to the correct class. Figure 5(a) presents an example in which the bird's pose is estimated incorrectly. After posing one question and re-evaluating attribute detectors for updated part probability distributions, our model is able to correctly predict the class.

In Figure 5(b), we visualize the question-asking sequence and how the probability distribution of part locations over the image changes with user clicks. We note in Figure 5(c) that our pose clusters did not discover certain poses, especially frontal views, and the system is unable to estimate the pose with high certainty.

As previously discussed, part click questions take on average less time to answer. We observe that the system will tend to ask 2 or 3 part click questions near the beginning and then continue with primarily binary questions (*e.g.* Figure 5(d)). At this point, the remaining parts can often be inferred reliably through reasoning over the spatial model, and thus binary questions become more advantageous.

7. Conclusion

We have proposed a novel approach to object recognition of fine-grained categories that efficiently combines class attribute and part models and selects questions to pose to the user in an intelligent manner. Our experiments, carried out on a challenging dataset including 200 bird species, show that our system is accurate and quick. In addition to demonstrating our approach on a diverse set of basic-level categories, future work will include introducing more advanced image features in order to improve attribute classification performance. Furthermore, we used simple mouse clicks to

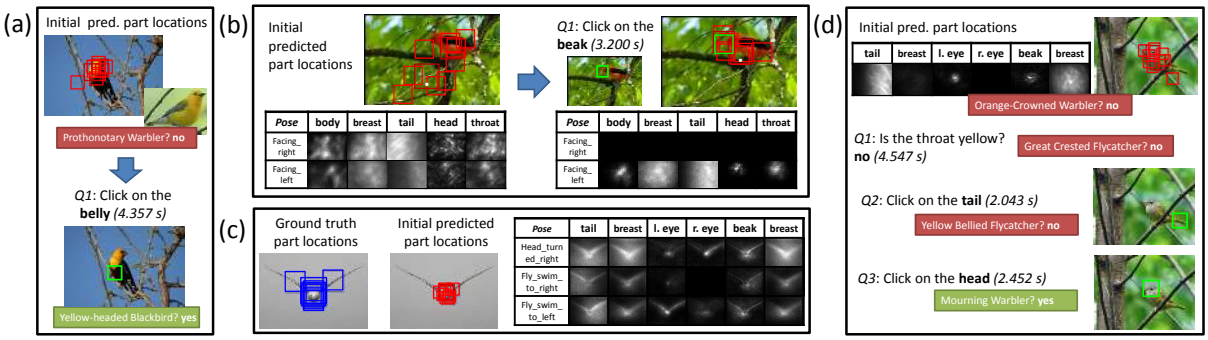

Figure 5. Four examples of the behavior of our system. 5(a): The system estimates the bird pose incorrectly but is able to localize the head and upper body region well, and the initial class prediction captures the color of the localized parts. The user's response to the first system-selected part click question helps correct computer vision. 5(b): The bird is incorrectly detected, as shown in the probability maps displaying the likelihood of individual part locations for a subset of the possible poses (not visible to the user). The system selects "*Click on the beak*" as the first question to the user. After the user's click, the other part location probabilities are updated and exhibit a shift towards improved localization and pose estimation. 5(c): Certain infrequent poses (*e.g.* frontal views) were not discovered by the initial off-line clustering (see Figure 2(a)). The initial probability distributions of part locations over the image demonstrate the uncertainty in fitting the pose models. The system tends to fail on these unfamiliar poses. 5(d): The system will at times select both part click and binary questions to correctly classify images.

designate part locations, and it would be of interest to investigate whether asking the user to provide more detailed part and pose annotations would further speed up recognition.

8. Acknowledgments

The authors thank Boris Babenko, Ryan Farrell, Kristen Grauman, and Peter Welinder for helpful discussions and feedback, as well as Jitendra Malik for suggesting time-to-decision as a relevant performance metric. Funding for this work was provided by the NSF GRFP for CW under Grant DGE 0707423, NSF Grant AGS-0941760, ONR MURI Grant N00014-08-1-0638, ONR MURI Grant N00014-06-1-0734, and ONR MURI Grant 1015 G NA127.

References

[1] P. Belhumeur et al. Searching the world's herbaria: A system for visual identification of plant species. In *ECCV*, 2008.

[2] L. Bourdev and J. Malik. Poselets: Body part detectors trained using 3d human pose annotations. In *ICCV*, 2009.

[3] S. Branson et al. Visual recognition with humans in the loop. In *ECCV*, 2010.

[4] I. Endres et al. The benefits and challenges of collecting richer object annotations. In *ACVHL*, 2010.

[5] A. Farhadi, I. Endres, and D. Hoiem. Attribute-centric recognition for cross-category generalization. In *CVPR*, 2010.

[6] A. Farhadi, I. Endres, D. Hoiem, and D. Forsyth. Describing objects by their attributes. In *CVPR*, 2009.

[7] L. Fei-Fei, R. Fergus, and P. Perona. A bayesian approach to unsupervised one-shot learning of object categories. In *ICCV*, volume 2, page 1134, 2003.

[8] P. Felzenszwalb et al. A discriminatively trained, multiscale, deformable part model. In *CVPR*, 2008.

[9] P. Felzenszwalb and D. Huttenlocher. Efficient matching of pictorial structures. In *CVPR*, 2000.

[10] A. Holub et al. Hybrid generative-discriminative visual categorization. *ICCV*, 77(1-3):239–258, 2008.

[11] N. Kumar et al. Attribute and simile classifiers for face verification. In *ICCV*, 2009.

[12] C. Lampert et al. Learning to detect unseen object classes by between-class attribute transfer. In *CVPR*, 2009.

[13] S. Lazebnik et al. A maximum entropy framework for part-based texture and object recognition. In *ICCV*, 2005.

[14] Martınez-Munoz et al. Dictionary-free categorization of very similar objects via stacked evidence trees. In *CVPR*, 2009.

[15] M. Nilsback and A. Zisserman. Automated flower classification over a large number of classes. In *ICCVGIP*, 2008.

[16] M. Stark, M. Goesele, and B. Schiele. A shape-based object class model for knowledge transfer. In *ICCV*, 2010.

[17] I. Tsochantaridis, T. Joachims, T. Hofmann, and Y. Altun. Large margin methods for structured and interdependent output variables. *JMLR*, 6(2):1453, 2006.

[18] C. Wah, S. Branson, P. Welinder, P. Perona, and S. Belongie. The Caltech-UCSD Birds-200-2011 Dataset. FGVC, 2011.

[19] M. Waite. http://www.whatbird.com/.

[20] G. Wang and D. Forsyth. Joint learning of visual attributes, object classes and visual saliency. In *ICCV*, 2009.

[21] M. Weber, M. Welling, and P. Perona. Unsupervised learning of models for recognition. In *ECCV*, Dublin, Ireland, 2000.

[22] P. Welinder et al. Caltech-UCSD Birds 200. Technical Report CNS-TR-2010-001, Caltech, 2010.

[23] Y. Yang and D. Ramanan. Articulated Pose Estimation using Flexible Mixtures of Parts. In *CVPR*, 2011.